CE597 Non-Linear Fracture Mechanics

2nd Term Project

Prof. Pablo Zavattieri

Fracture toughness test and its simulation for brittle and ductile steel

2011. 4.29.

Min-Kwang Choi

Tae-Hwan Kim

Chiara Villani

1. Introduction

For ductile materials, the usual design procedure is based on the yield point stress, but if the material is prone to fracture the approach has to be different. In this case, in particular, we can divide into three phases:

- Choice of the maximum size crack that the material has to be able to tolerate without fracturing. It is usually done by visual inspection and it is selected on the basis of the sensitivity of the inspection done.
- Calculation of the level of stress with which such a crack can coexist;
- Based on the stress evaluated in the previous point, evaluation of the load that can be carried by the structure analyzed.

It is obvious that the second phase will be the most challenging, since most of the materials are not simply linear and then the equations based on Griffith theory are not applicable anymore. More in detail, the evaluation of stress will be function of the dimensions of the loaded material and of the circumstances of loading.

In the common practice, how is then possible the evaluation of the state of stress that can be tolerate by a certain material? For metals, until last year there was an ASTM standard that allowed the calculation of the material sensitivity in presence of cracks. ASTM 338 "Sharp Notch Tension Testing of High-Strength Sheet Materials" was providing information on the level of stress that can be tolerated by a certain material in the presence of a crack running a uniaxial tension test on a thin sheet in plane-stress condition. However, this test was presenting several limitations since the results are dependent upon the geometry and the sharpness of the notch, therefore it only gives relative data useful to compare materials. This is probably the reason why it has been withdrawn recently (2010).

In this project, our focus was on the test mentioned above: we have indeed tested two different kind of steel (brittle and ductile) in order to show their different response to the crack propagation.

This phase was then followed by the modeling and simulation of the experiments through the software ABAQUS. The comparison among experiments and simulation was finally analyzed.

2. Experimental details and results

2.1 Materials

As previously mentioned, in order to see the resistance to crack propagation in steel specimen, two different steels have been tested according to ASTM 388 "Sharp Notch Tension

Testing of High-Strength Sheet Materials". In particular the following types of steel have been used in our experiments:

- *Ductile Steel* : 1018, hot rolled, mild;
- *Brittle Steel* : 1090, cold drawn and annealed.

The reference properties of the materials used are summarized in Table 1 and 2.

Table 1. Properties of ductile steel

DUCTILE STEEL 1018		
Chemical composition: C=0.15-0.20%, Mn=0.60-0.90%, P=0.04% max, S=0.05% max		
Density	0.284	lb/in³
Modulus of elasticity	29000	ksi
Tensile strength (hot rolled)	58000	psi
Yield strength (hot rolled)	31900	psi
Elongation (hot rolled)	36	%
Hardness (hot rolled)	66	RB

Table 2. Properties of brittle steel

BRITTLE STEEL 1090		
Chemical composition: C=0.90%, Mn=0.75%, P=0.04% max, S=0.05% max		
Density	0.284	lb/in³
Modulus of elasticity	29000	ksi
Tensile strength (hot rolled)	122000	psi
Yield strength (hot rolled)	66700	psi
Elongation (hot rolled)	10	%
Hardness (hot rolled)	98	RB

In order to see the influence of the presence of the crack in the material response under uniaxial tension load, two samples with different geometry have been tested:

- Unnotched sample (Figure 1)
- Notched sample (Figure 2)

The dimensions of the samples are summarized in Table 3.

Table 3. Geometry of the samples

	Height [in]	**Width** [in]	**Thickness** [in]
Unnotched sample	2	2	0.125
Notched Sample	2	2	0.125

Figure 1. Un-notched steel plate

Figure 2. Notched steel plate

2.2 Test Procedures

As suggested in the ASTM 338, the sample is loaded under uniaxial tension until failure occurs with constant displacement rate 0.002 in/min. The sample was tensioned by a servo-hydraulic machine (Figure 3).

The displacement has been recorded by means of LVDT of length 2 in (Figure 4), which was fixed directly on the steel specimen in order to obtain the real displacement. During the test, the applied load on the steel specimen was also recorded along with displacement.

Figure 3.Servo-hydraulic machine for tension test

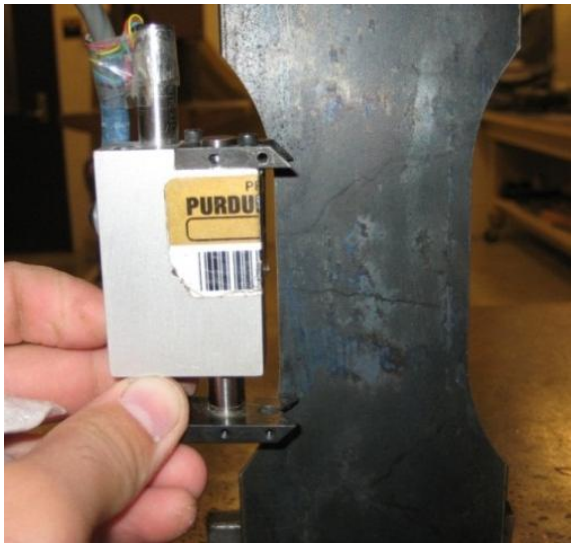

Figure 4. Installation of LVDT

2.3 Results

2.3.1 Observation of failure

The appearance of the samples after the test is shown in Figure 5 and 6. In particular we should notice the difference in the fracture surface between brittle and ductile samples: the former has indeed very sharp edges that prove the absence of plastic deformation during crack propagation. The opposite can be seen instead in the case of ductile steel: here the edges of the crack surface are smoother and the section of the sample appears restricted. Moreover, the central part of the sample is lighter and the grid is substantially deformed. All these aspects testify the occurrence of plastic deformations during the test.

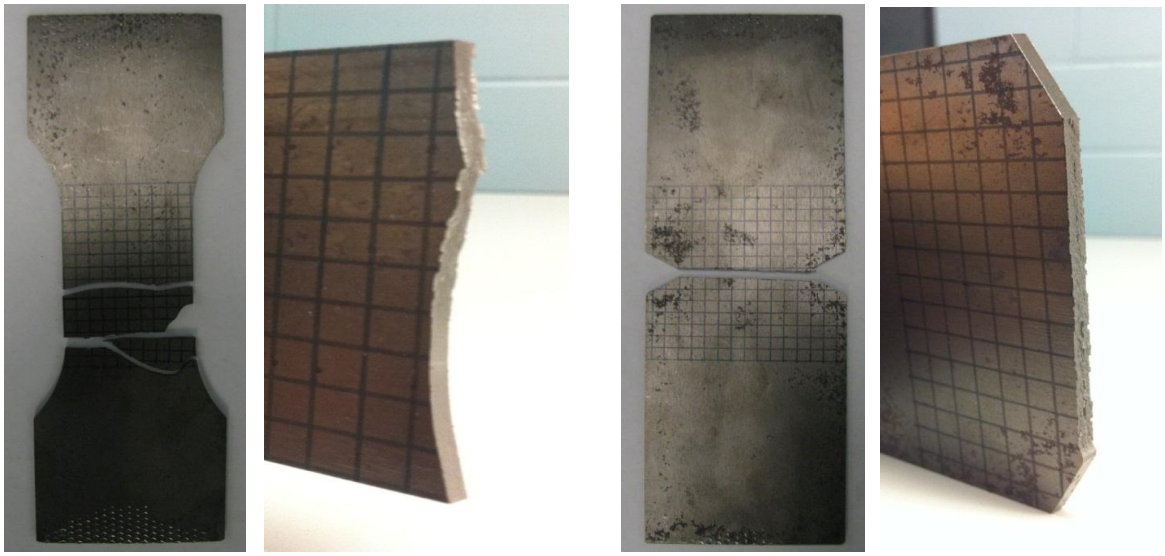

Figure 5. Fracture surfaces brittle steel samples (Left: un-notched, right: notched)

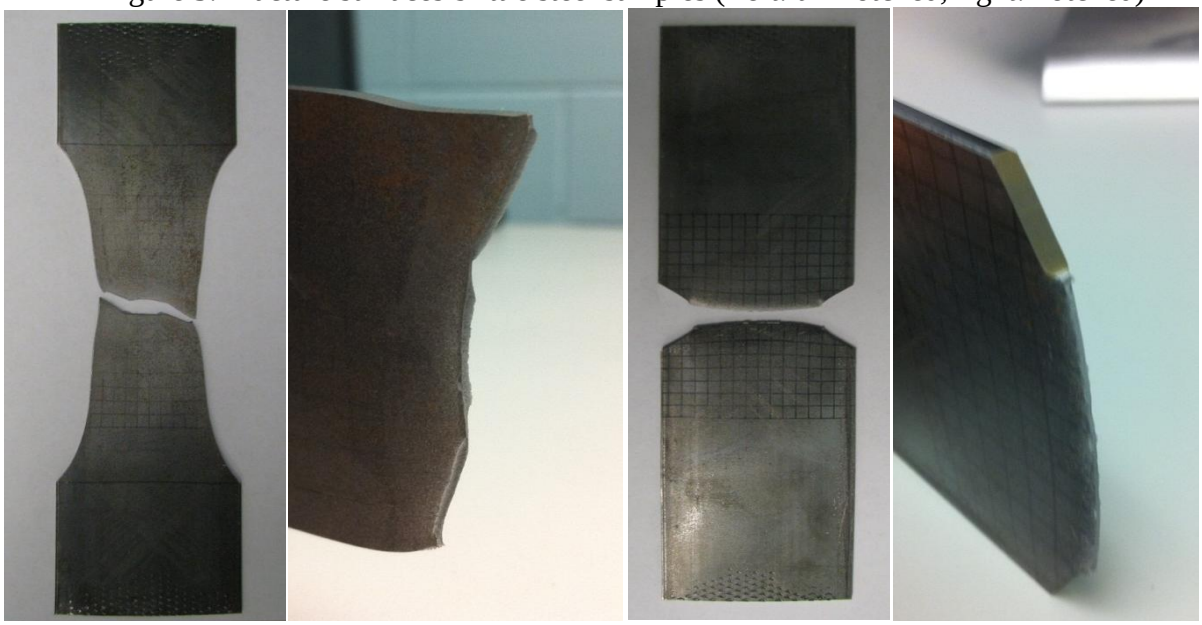

Figure 6. Fracture surfaces brittle steel samples (Left: un-notched, right: notched)

2.3.2 Analysis

Experimental data, displacement–load curve, obtained from the servo-hydraulic machine were analyzed. Figure 8 shows the force and displacement curves for all steel plates.

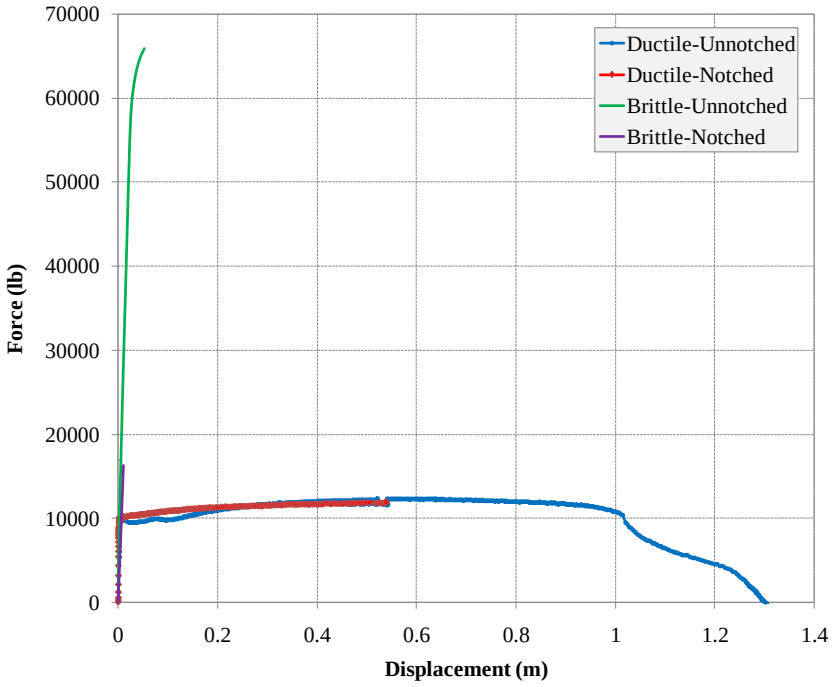

Figure 8. Force and displacement for all steel plates

The ultimate load of notched and un-notched ductile steel plates is around 11800 lb. The existence of notch does not affect the ultimate load that the sample can resist. However, the plastic deformation of the ductile notched plate (DNP) was much smaller than the ductile un-notched plate (DUNP). The brittle un-notched plate (BUNP) had about 65000 lb of the ultimate load. However, the brittle notched plate (BNP) had the much smaller ultimate load (15700 lb) than the BUNP. These results revealed that the brittle material is much more notch-sensitive than the ductile material. In addition, brittle material had very small plastic deformation and suddenly failed.

The properties of steel plates were analyzed and summarized in Table 4. The elastic modulus obtained from the experiment is smaller than the reference values in the Table 1 and 2. In addition, the modulus elastic of DNP from the experiment was unreasonable high value. In this report, that high value was regarded as experimental error and the authors assume that the elastic modulus of DNP is equal to the value of DUNP. The BNP also showed the relatively smaller elastic modulus than the BNUP though those values should be more or less equal theoretically. These errors of elastic modulus seem to be caused by the poor installation of the LVDT. In the experiment, to fix the LVDT, the rubber bands were used and positioning the LVDT was also

performed without the precise consideration. This poor installation of LVDT might results in the errors for measuring the displacement. This error should yield the erroneous elastic modulus since the elastic modulus is computed using the initial small displacement which is more easily affected by the installation of LVDT.

ASTM 338 provides the calculation of the material sensitivity in presence of cracks. The specification allows us to calculate the ratio of the ultimate strength in the notched steel plate (SNS) to the yield stress in the un-notched steel plate (YPS). If this ratio is close to one, the material is not notch sensitive and is resistant to be cracked. If the ratio is much less than one, the material is notch sensitive and the existence of notch results in the significant reduction of the ultimate strength. The ratio (SNS/YPS) was computed and is shown in Table 4. As the specification was explained, the ratio for ductile material is 1.34 which is close to 1 and the ratio for brittle material is 0.26 which is far less than 1.

Table 4. Properties of the steel plates

Metal	Properties				
	Elastic Modulus [psi]	Yield Strength [psi]	Ultimate Strength [psi]	Poisson Ratio [-]	SNS/YPS
DUNP	$2.05*10^7$	41000	63700	0.28	1.34
DNP	$2.05*10^7$	43000	54800	0.28	
BUNP	$2.1*10^7$	236000	270000	0.28	0.26
BNP	$1.5*10^7$	-	61600	0.28	

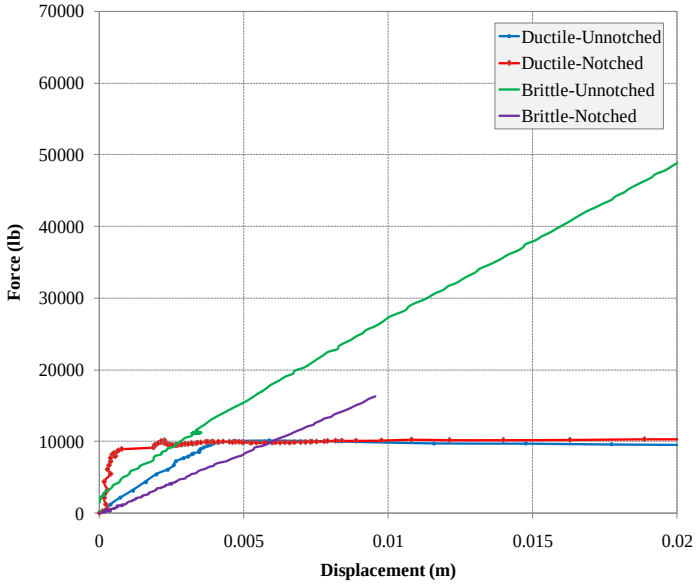

Figure 9. Force and displacement curves for all plates (magnifying the initial period)

3. Cohesive element

Cohesive element has been the most relevant way to model interfacial problems since Barenblatt(1959,1962) firstly proposed it. We can build a numerical model to simulate failure of adhesive material between two rigid or deformable bodies, interfacial debonding behavior of two contacted surfaces, or crack propagation at bonded interface. The behavior of cohesive model is governed by traction-separation law. Generally, it is known that there are two dominant parameters for cohesive element, the maximum stress that a cohesive element can hold without failure (σ_{max}) and separation work done by separation displacement (Γ_0) (Xu & Needleman(1994) and Tvergaard & Hutchinson (1992)). In some case, the shape of traction-separation law (T-δ) can dominate macroscopic behavior of a numerical model (Chandra et al (2002)).

3.1 Traction-separation laws

ABAQUS standard/explicit provides three types of traction-separation law, triangular, exponentially softening, and user defined softening models, as shown in Figure 9. The most popular model among these three traction-separation laws for cohesive element is triangular traction-separation law. It is simply defined with elastic stiffness (κ), strength of an element (σ_{max}), and critical displacement at failure (δ_c). In the triangular model, applied stress on cohesive element increases with the slope of κ upto the strength of the element (σ_{max}) and decays linearly till the displacement of the element reaches to critical displacement (δ_c).The critical energy release rate of this model can be easily calculated by getting the area under the traction-separation curve. Exponentially softening model behaves in the same way before the strength (σ_{max}). Once the applied stress reaches to the strength, then the strength of the cohesive element decreases exponentially with increasing displacement. In ABAQUS, the level of softening is defined by the damage variable D and the reduced strength is calculated by the following equations. For user defined softening model, damage variable can be directly input with corresponding displacement.

For triangular model,

$$D = \frac{\delta_c(\delta^{\max} - \delta_m)}{\delta^{\max}(\delta_c - \delta_m)}$$

For exponentially softening model,

$$D = 1 - \left\{\frac{\delta_m}{\delta^{\max}}\right\}\left\{1 - \frac{1 - \exp\left(-\alpha\left(\frac{\delta^{\max} - \delta_m}{\delta_c - \delta_m}\right)\right)}{1 - \exp(-\alpha)}\right\}$$

where, δ_c is the critical displacement at failure, δ_m is the displacement when the applied stress reaches to the strength (σ_{max}), δ^{max} is the maximum displacement attained after δ_m, and α is the non-dimensional material parameter that defines the rate of damage evolution.

Reduced strength (σ^r_{max}) of cohesive element is defined as,

$$\sigma^r_{\max} = \sigma_{\max}(1 - D)$$

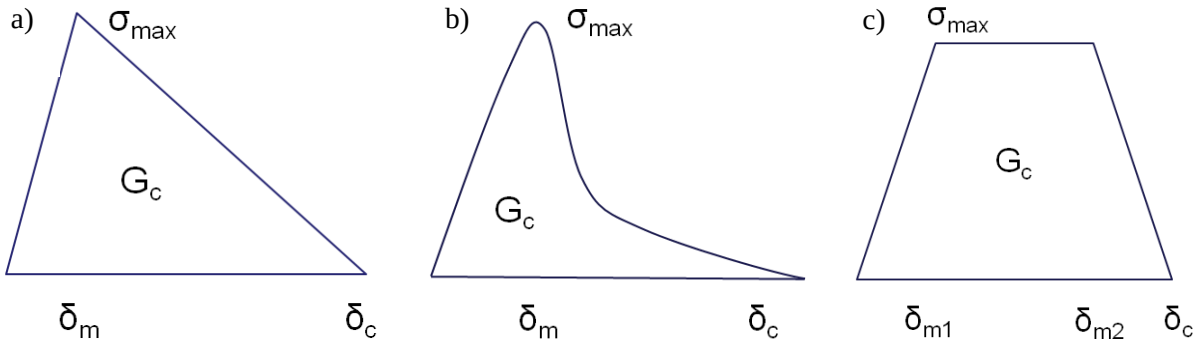

Figure 9. Traction-separation laws propvided in ABAQUS, a) triangular, b) exponentially softening, and c) user defined softening models.

3.2 Modeling technique for cohesive behavior

ABAQUS provides users two ways of modeling method for cohesive behavior; 1) handling contact problem at the interface which is governed by cohesive behavior and 2) inserting cohesive element between rigid or deformable solid elements. Main advantage of the first option is that the thickness of interface can modeled to be zero so that the effect of element thickness can be neglected. Inserting cohesive element between solid elements has an advantage that user can visually see the variation of displacement, stress, failure, and crack propagation of the cohesive element. It should be noted in the second method that ABAQUS consider the thickness of cohesive element to calculate the stiffness of interface, which is calculated by the following equation.

$$\kappa_{interface} = \frac{E_c}{t_c}$$

where $\kappa_{interface}$ is the stiffness of interface relating the normal traction to the displacement at the interface, E_c is the stiffness of cohesive element and t_c is the thickness of cohesive element.

In our numerical models, the second modeling technique is adapted to simulate crack growth of notched or unnotched samples and the thickness of cohesive element is assumed to be 10^{-4} inches, which is the recommendation of ABAQUS Manual to avoid numerical problems.

3.3 Selection of traction-separation law

Traction-separation law for numerical models is determined by trial and error. Triangular traction-separation law was simply chosen for brittle steel plate in the first trial because the shape of load-displacement curve obtained from the experiment on it is triangular. The strength of cohesive element is assumed to be yield stress taken from corresponding experiment data. During trial and error process, it was found that solution procedure of ABAQUS became very unstable if δ_m is close to δ_c, which means very brittle failure. Time increment to solve the model approaches to almost zero. Finally, exponentially softening traction-separation law was employed to numerical models for brittle steel plate and showed good stability during solution. Model parameters for cohesive element were calibrated by trial and error till the model can

produce the similar load displacement curve comparing with experimental data. For ductile steel plate, cohesive element is employed for only notched sample. From the experiment results, it showed relatively larger post-yield displacement that brittle steel plate. Therefore we design the cohesive element to have large critical displacement δ_c. The calibrated traction-separation laws of cohesive element are shown in Figure 10.

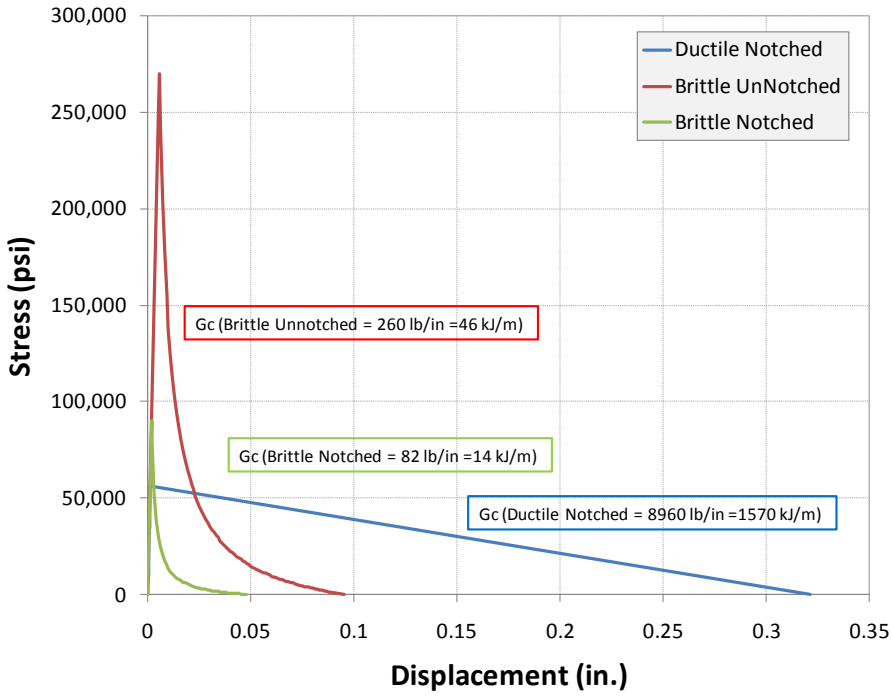

Figure 10. Calibrated traction-separation laws for ductile steel plate with notch and for brittle steel plate with and without notch.

4. Simulation and Comparison with Experimental Results

This chapter is divided three consecutive subchapters; details of modeling, results of simulation and analysis of simulation results and experimental results. The first subchapter includes details of modeling procedure to simulate including the model geometry, mesh type, property of cohesive element and details of loading. Then, second subchapter provides the simulation results. Then, in the last subchapter, analysis between the simulation results and the experimental results will be discussed.

4.1 Details of Modeling

All steel plates (DNP, DUNP, BNP and BUNP) were modeled by using non-linear software, ABAQUS. The summary and conditions of modeling are as follows.

- Due to the geometric symmetry of steel plates, only right part of the steel plate was modeled
- All material used in these models is homogeneous, isotropic, elastic and plastic. The plastic deformation was introduced into the ABAQUS program as a tabular type data obtained from the experimental results.
- Large deformation is considered by using command NLGEOM.
- For DNP, DUNP and BNP, 3 node triangular element (CPS3) was used and the geometric order of element is linear. For BUNP, 4 no de bilinear quadrilateral (CP4R) element was used.
- Cohesive element was inserted to the model of DNP, DUNP and BNP to be cracked. The thickness of cohesive element (10^{-4} in) was considered and these cohesive elements were connected to the bulk material with "Tied constrained".
- Horizontal displacement (U1) for the left side and vertical displacement (U2) for the bottom side was constrained as a boundary condition. Then, the constant displacement velocity was applied to the top side of the model. Therefore, this model can simulate the displacement controlled condition.

The mesh generations of each steel plate are shown in Figure 11 and the parameters used in the simulation are summarized in Table. 5. Ductile steel plate had large plastic deformation and thus it took a longer time till reaching the completely failure, while the brittle steel plate took relatively short time till failure. Therefore, the displacement rates were determined by considering those effects as shown in Table 5.

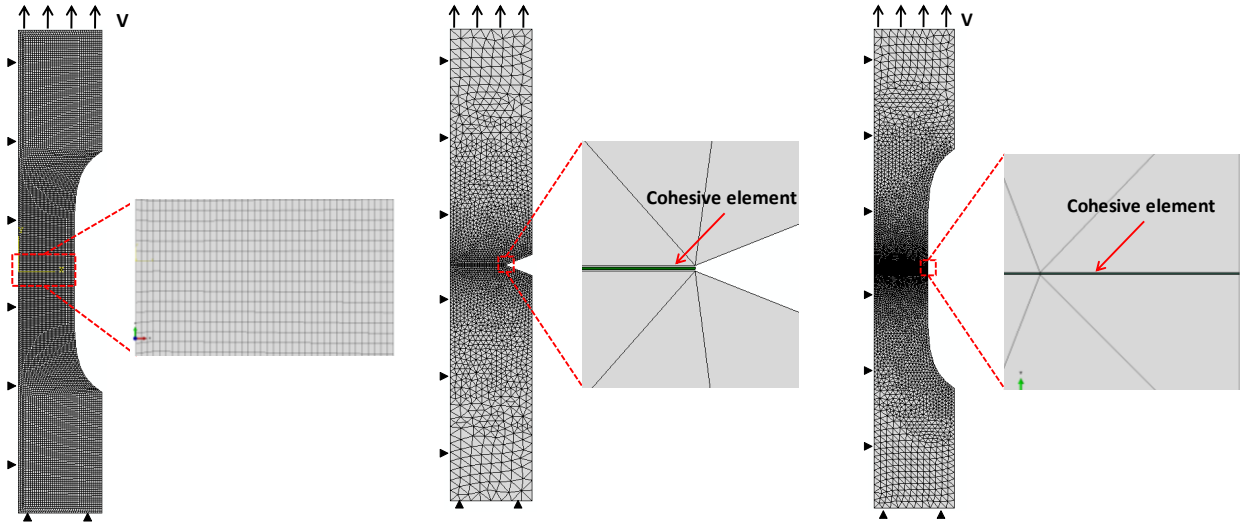

(a) (b) (c)

Figure 11. Mesh generations; (a) DUNP, (b) DNP and BNP, (c) BUNP

Table 5. Properties of mesh and displacement control

Metal	Mesh generation and Displacement			
	Mesh type	Cohesive element	Rate	Rate
DUNP	CP4R (4 node bilinear quad)	X	V=0.01 in/s	T=200 s
DNP	CPS3 (3 node linear tri)	O (10^{-4} in)	V=0.01 in/s	T=100 s
BUNP	CPS3 (3 node linear tri)	O (10^{-4} in)	V=0.001 in/s	T=200 s
BNP	CPS3 (3 node-linear tri)	O (10^{-4} in)	V=0.0001 in/s	T=500 s

4.2 Results of simulation

4.2.1 Ductile un-notched steel plate (DUNP)

Ductile un-notched steel plate did not use the cohesive element because simulating the model with the cohesive model did not well agree with the experimental results. The main reason of this disagreement is caused by the softening behavior of ductile steel plate. If the strength of cohesive element is higher than the ultimate stress of the ductile steel plate, it just

stay in the elastic region, while if the strength is lower than the ultimate stress, the cohesive model start to show post-peak softening behavior before the steel reach its ultimate stress. Therefore, when using the cohesive element, capturing the softening behavior of the ductile steel is really difficult. Finally, for simulating the DUNP, the cohesive element was not applied.

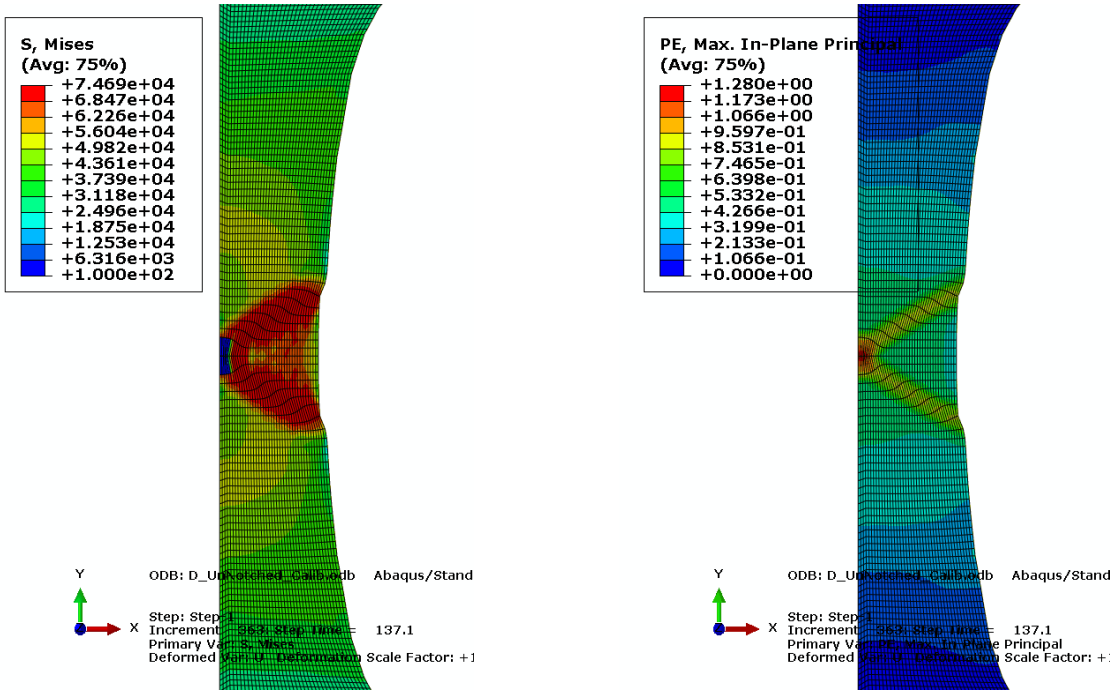

(a) (b)

Figure 12. Results of simulation; (a) Von Mises stress, (b) Plastic maximum in plane principal strain

Figure 12 shows the results of the simulation in terms of Von Mises stress and plastic maximum in plane principal strain. Figure 12(a) shows that the area at the center of the plate loses the resistance of stress and starts opening the crack (blue colored area). The interesting thing is the distribution of the stress in the middle of the plate. The high Mises stresse are distributed along the inclined line from the center of the plate to the right boundary of the mesh (colored red zone in Figure 12 (a)). This implies that the crack will propagate along this inclined line which has the higher stress distribution. In addition, the maximum plastic strain also shows the similar distribution. The center of the plate has the largest plastic deformation and the inclined lines colored by yellow are the second highest plastic deformation. Therefore, this

distribution of the stress and strains explain why the crack obtained by experiment started opening in the center and propagated along the inclined line as shown in Figure 6.

4.2.2 Ductile notched steel plate (DNP)

Ductile notched steel plate (DNP) used the cohesive model and the results shows very similar behavior of the experimental results. Unlike the DUNP, when DNP reached ultimate stress, it drastically lost the stress resistance and failed. The previously observed difficulty for DUNP did not affect on the DNP model. Therefore, the simulation successfully described the crack propagation with cohesive model.

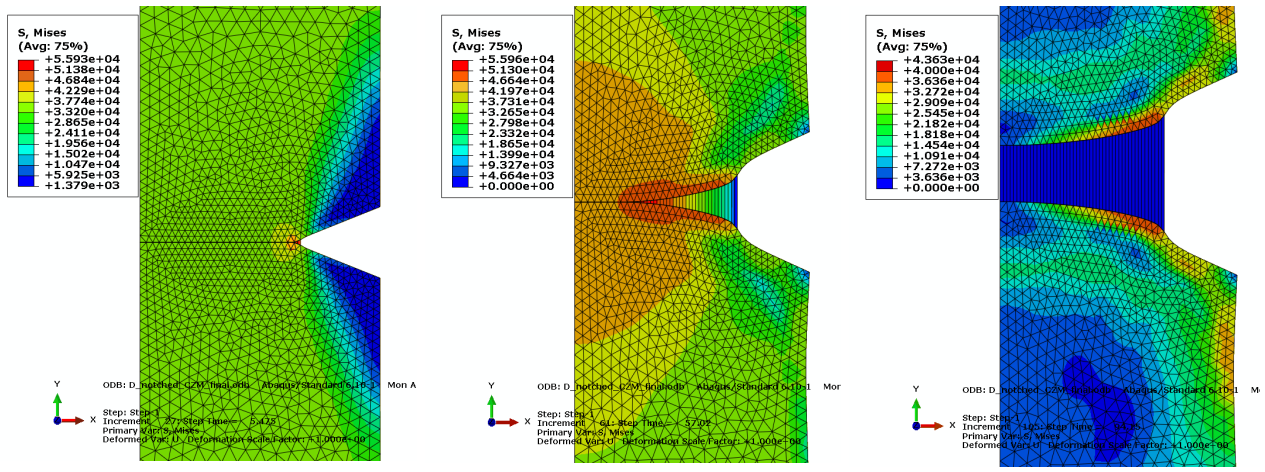

(a) Step 1 (b) Step 2 (c) Step 3

Figure 13. Von Mises stress near the notch; (a) at vertical displacement=0.058 in, (b) at vertical displacement=0.565 in and (c) at vertical displacement=0.942 in

Figure 13 shows the Von Mises stress distribution near the notch at each step (vertical displacement of top = 0.058 in., 0.565 in. and 0.942 in. respectively). Step 1 in Figure 3 (a) is the moment when the first cohesive element reached to its strength. Due to the stress concentration, the highest stress occurs in the tip of the notch and the cohesive element at the tip starts opening while losing the stress. Step 2 shows the crack propagation while loading. The stress distribution is clearly observed along the cohesive model. Toward the crack tip, the stress in cohesive element reduces and the blue region indicates that there is no resistance because the displacement of this element exceeds the critical displacement that was defined by traction-

separation law. Step 3 is the moment when the DNP failed completely. All cohesive elements deliver no stress as shown in Figure 13 (c). The deformed shape is more or less identical with the experimental result in Figure 6.

4.2.3 Brittle un-notched steel plate (BUNP)

The BUNP failed drastically when it reached the highest stress without softening. This is because it has small plastic deformation that is opposite to the case of the ductile plates.

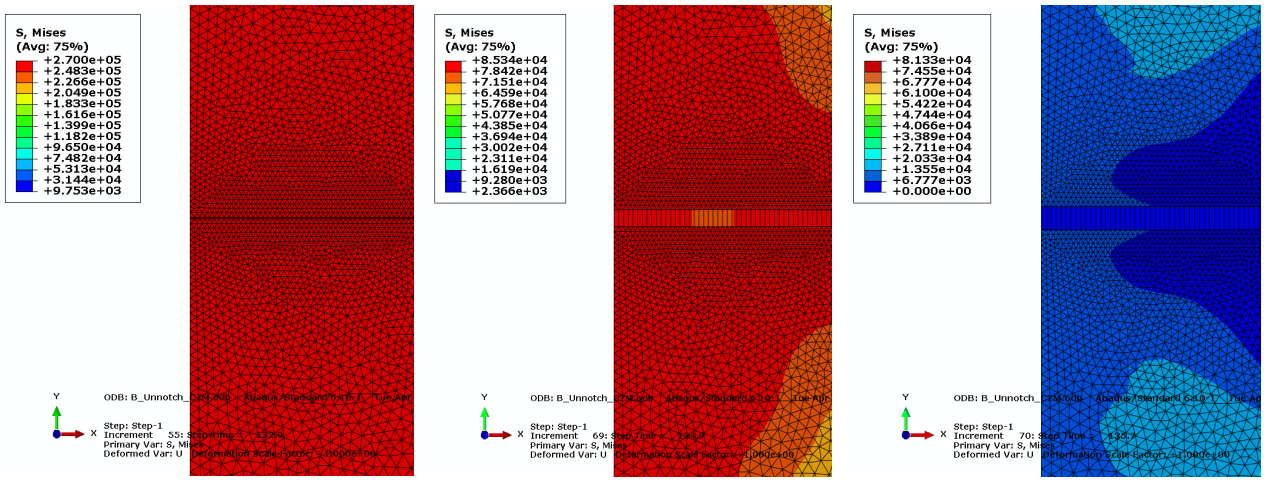

(a) Step 1 (b) Step 2 (c) Step 3

Figure 14. Von Mises stress near the notch; (a) at vertical displacement=0.133 in, (b) at vertical displacement=0.135 in and (c) at vertical displacement=0.136 in

Figure 14 shows the Von Mises stress distribution near the notch at each step (vertical displacement of top = 0.133 in, 0.135 in. and 0.136 in. respectively). Step 1 in Figure 14 (a) is the moment when the DUNP reaches the maximum stress. Lack of notch causes the uniform stress distribution over the DUNP. Once the applied stress reaches to the strength of cohesive element, the cohesive element exhibits the softening behavior as shown in Figure 10 and the strength goes to nothing. During this period, the deformation of cohesive element significantly increases while the bulk material is placed under the unloading condition. This phenomenon is similar to the localization of the steel plate. In this project, the cohesive element was embedded in the middle of the plate, and thus this localization occurs along the cohesive element. Step 2 in Figure 12 (b) is the moment just before the failure of cohesive element. After this step, the

failure suddenly occurs and all cohesive elements lose their strength simultaneously. This phenomenon is well coincident with the sudden failure in the experiment.

4.2.4 Brittle notched steel plate (BNP)

The BNP failed suddenly at the much lower stress than the BUNP due to the stress concentration near the notch. Most of bulk steel materials were under the elastic region when failure occurred because the stress at failure was very small.

Von Mises stress distribution near the notch is shown in Figure 15 at each step (vertical displacement of top=0.012 in. and 0.020 in. respectively). Step 1 in Figure 15 is the moment when the cohesive element reaches its strength. After this point, the strength of cohesive element starts to be softened and the neighbor cohesive model can reach upto its strength. Finally, before the failure of bulk steel material, we can observe the failure propagation of cohesive element as shown in Figure 15 (b). This consecutive failure of cohesive element can successfully explain the sudden failure of notched brittle steel sample under low load with small displacement.

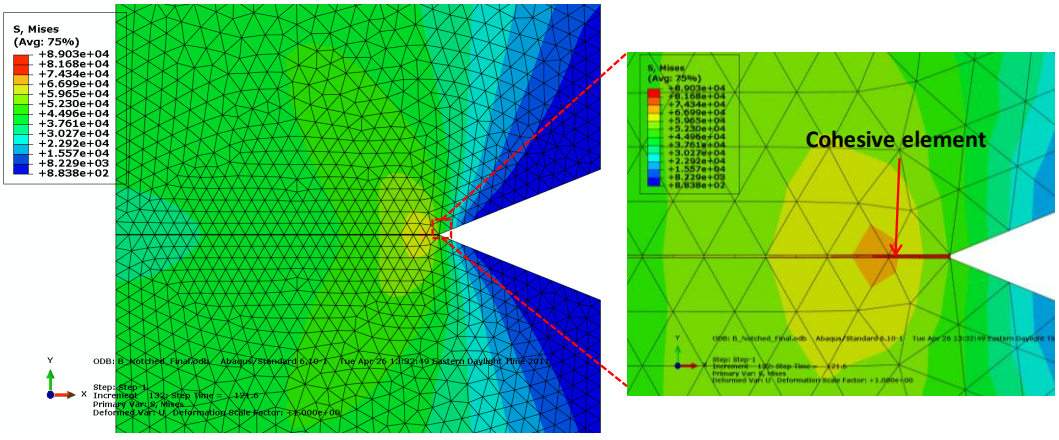

(a) Step 1

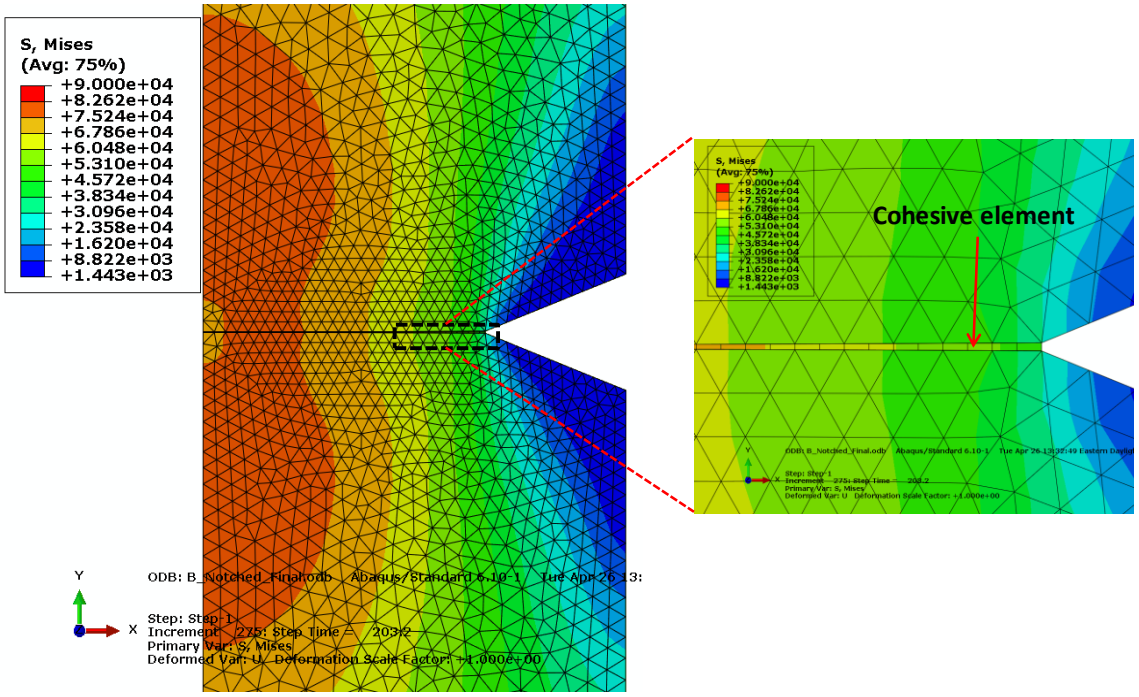

(b) Step 2

Figure 15. Von Mises stress near the notch; (a) at vertical displacement=0.012 in and (b) at vertical displacement=0.020 in

4.3 Analysis of simulation results and experimental results

This section will compare the simulation results with the experimental results. First of all, the ductile steel plate (DUNP and DNP) will be considered and then the brittle steel plate (BUNP and BNP) will be analyzed.

4.3.1 Ductile steel plate (DUNP and DNP)

Figure 16 shows the force and displacement curves for ductile steel plate (DUNP and DNP) obtained from the simulation and the experiment.

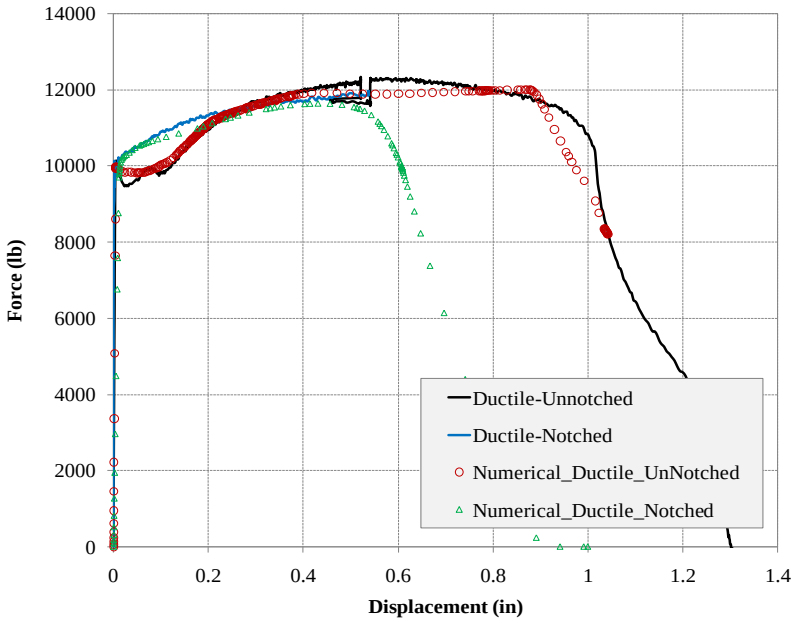

Figure 16. Force and displacement curve for simulation results and experiemental resutls of ductile steel plate

As shown in Figure 16, the simulation results well trace the experimental data. For DUNP, simulation data can not exactly describe the ultimate stress and the slight softening which occurs in experimental data. It might be difficult to simulate the softening effect by using the typical mesh. Applying the adaptive mesh in softening steps might provide more reasonable simulation results. However, the simulation results are more or less identical with the experimental data and the simulation well describes the opening of crack and the potential propagation of the crack as shown in section 4.2.1. In the case of the DNP, the simulation shows the very similar behavior to the experimental data. The cohesive elements successfully capture the failure of the sample.

It is observed that the ductile plate shows the more or less identical behavior with/without the notch. This means that the ductile plate is not notch sensitive and it has the resistance to be cracked even though it has a notch. The large plastic deformation and energy dissipation for this plastic deformation reduce the amount of the stress concentration near the crack tip and thus the notch cannot severely affect the behavior of the ductile steel plate before DNP failures.

However, DNP reduces the amount of the post yield deformation. The stress concentration near the notch causes more plastic deformation in that region even though the bulk material still in the

elastic region. Thus, the potential plastic deformation near the notch has been used up before the general yielding occurs in the bulk material. This pre-yielded region near the notch starts softening earlier and thus cracks propagate along this region. The total deformation of DNP greatly reduces for this reason.

4.3.2 Brittle steel plate (BUNP and BNP)

The behavior of the brittle steel plate is very different from the behavior of the ductile steel plate. Since the brittle steel plate has very small plastic deformation, it showed brittle failure and the displacements at failures are also much smaller than the ductile steel plate (DUNP = 1.3 in, DNP = 0.6 in, BUNP=0.055 in and BNP = 0.008 in) as shown in Figure 17. In addition, the ultimate stress of BNP is much smaller than the one of BUNP unlike the case of the ductile plate. The small plastic deformation that is a distinct character of brittle steel results in fast propagate at the lower stress.

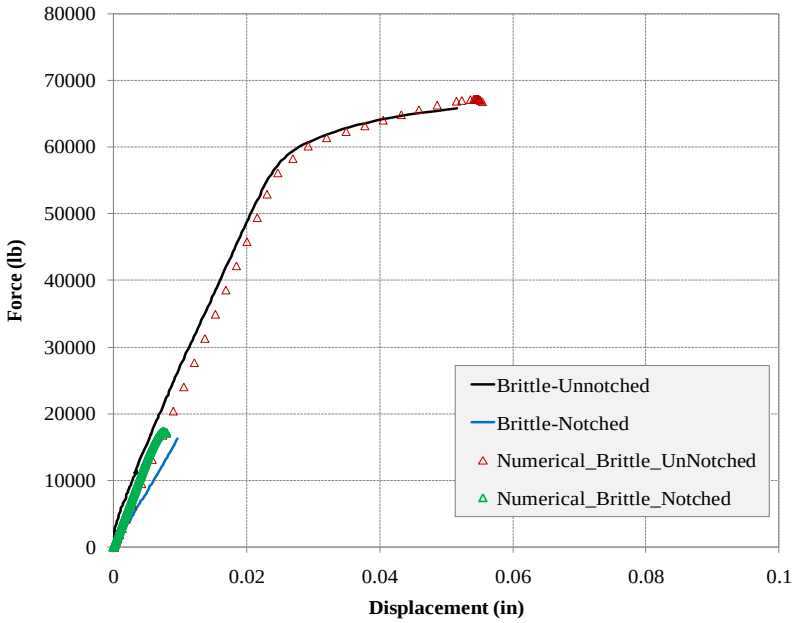

Figure 17. Force and displacement curve for simulation results and experiemental resutls of brittle steel plate

5. Conclusions

The experimental analyses for the ductile and brittle steel plate with/without notch were performed. In addition, the numerical analyses also conducted by using the ABQUS software. Overall comparison between the experimental and numerical analyses reveal that cohesive element can be successfully applied to model the failure induced by crack propagation

The following results are drawn through this project.

- Elastic modulus obtained from experiments showed the large variation. This seems to be caused by the poor installation of the LVDT. In order to obtain more accurate data, the installation of the LVDT should be very important.
- Notched samples whether the sample is ductile or brittle, experience smaller post yield displacement.
- Brittle steel plate exhibits higher notch sensitivity (SNS/YPS=0.26) while ductile steel plate is not notch sensitive (SNS/YPS=1.34)
- Based on test results, Brittle steel (1090) can be placed on the LEFM region and ductile one (1018) on the strength-base area
- Cohesive element is applied to simulate the failure of brittle steel, as well as of ductile steel with high stress concentration
- Calibrated cohesive model for brittle (1090) and ductile (1018) steel is obtained
- Critical energy release rate (G_c) of ductile is much higher than the brittle one.
- Numerical simulation shows good agreement with experiment results